# Digital heterodyne interference fringe control system

Ralf K. Heilmann,[a] Paul T. Konkola, Carl G. Chen, G. S. Pati, and Mark L. Schattenburg
*Space Nanotechnology Laboratory, Center for Space Research, Massachusetts Institute of Technology, Cambridge, Massachusetts 02139*

(Received 15 June 2001; accepted 20 August 2001)

In traditional interference lithography, interference fringes are typically phase locked to a stationary substrate using analog homodyne photodiode signals that are fed back to control a phase-shifting device such as an electro-optic modulator or a piezoelectrically transduced mirror. Commercially available fringe-locking systems based on this approach often achieve stability of the interference fringes to within a small fraction of the fringe period $p$ (typically $\pm p/20$ peak-to-peak). We describe the performance of a heterodyne fringe control system utilizing acousto-optic phase shifters and digital controls that is designed to satisfy the much more stringent fringe control requirements for scanning beam interference lithography. We demonstrate locking to $\pm p/100$, and expect further significant improvements. This versatile system can also be used to lock the phase of moving fringes in almost arbitrary fashion at fringe velocities up to $2.5\times10^7$ periods/s and to measure the phase of gratings. © *2001 American Vacuum Society.* [DOI: 10.1116/1.1410096]

## I. INTRODUCTION

Whenever a holographic exposure takes more than a small fraction of a second, fluctuations in the index of refraction of the air traversed by interfering laser beams, as well as vibrations and thermal drifts, can introduce changes in the optical path-length difference between the beams. These changes lead to motion in the interference pattern, which degrades the contrast in the resulting exposure. In order to minimize fringe movement one can implement a feedback system that detects the phase of the fringe pattern and actuates a phase-shifting device in the path of one of the interfering beams.[1] Such fringe lockers have been used for decades and typically limit fringe drift to $\pm 1/20$th of a fringe period $p$.[2] A number of phase-modulation techniques[3–6] have improved on different aspects of phase control for specific applications in the past.

Popular choices for phase shifters are opto-electronic modulators (Pockels cells) and piezo-mounted mirrors. While the former have a large bandwidth, their phase range is limited to $\approx 2\pi$. Piezoelectric transducers can achieve many multiples of $\pi$ in phase change, but they are relatively slow. In contrast, acousto-optic modulators (AOMs) or Bragg cells offer infinite phase range and transit times on the order of 100 ns.[7] Nevertheless we are not aware of any previous fringe control application that uses AOMs as actuators.

In our system acousto-optic phase shifting also enables straightforward conversion of relatively low-frequency phase error signals into high-frequency heterodyne signals. Compared to the homodyne case, heterodyne detection offers better signal-to-noise ratios, reduced sensitivity to differential amplitude variations, and less drift due to $1/f$ noise.[8,9] Furthermore, fast, high-resolution, low data-age, and low data-age uncertainty digital phase measuring electronics with large bandwidth are readily available for heterodyne signal processing.[10]

All of these features are essential for scanning-beam interference lithography (SBIL),[11,12] a technique currently under development in our laboratory. Its basic premise is to generate large area ($\approx$300 mm diameter) phase-coherent fiducial gratings and grids by scanning a resist-coated substrate through an ultralow distortion interference pattern (with diameter $d\approx 1$ to 2 mm) formed by two narrow laser beams. Since the substrate is mounted to a moving stage the fringes need to be locked to the moving substrate, i.e., we not only require the ability to lock the fringes, but to move them in a controlled manner.

In the most basic scheme the substrate is scanned through the interference pattern in the direction parallel to the interference fringes at some speed $v$ [see Fig. 1(a)]. Fringe drift at frequencies much greater than $v/d$ will reduce the contrast in the recorded pattern. For these frequencies we consider locking to $\pm p/100$ as sufficient. At smaller frequencies fringe drift will lead to meandering grating lines. For metrology applications[11] we want to limit the latter deviations to 1 nm or less, e.g., we require stability of $\pm p/2000$ for a grating period $p$ of 2 $\mu$m, while $\pm p/200$ would be sufficient for $p = 200$ nm.

In a more advanced scheme the substrate would be scanned at an arbitrary angle relative to the interference fringes [see Fig. 1(b)]. This necessitates a continuously increasing phase difference between the two interfering beams in order to lock the pattern to the substrate. The easiest way to achieve this is for the beams to have different frequencies. AOMs are the natural choice for this task.

## II. SYSTEM SETUP

A schematic of our system setup is shown in Fig. 2. A cw laser beam ($\lambda = 351.1$ nm, frequency $f_0 \approx 854$ THz) is incident onto the acousto-optic modulator AOM3, which splits off a weak first-order reference beam with frequency $f_R = f_0 + 120$ MHz (gray line in Fig. 2). The undiffracted zeroth-order beam is then split by a grating beam splitter,

[a]Electronic mail: ralf@space.mit.edu

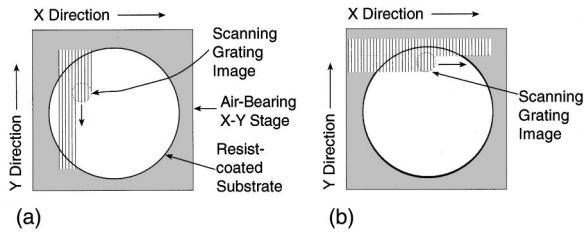


FIG. 1. SBIL scheme for writing large-area gratings. (a) Scanning parallel to the lines in the interference pattern. (b) Scanning in the direction perpendicular to (a). The interfering beams are in the *x*-*z* plane (not shown).

ideally with twice the period of the desired interference pattern.[13] Each of the two first-order beams then propagates through another AOM (AOM1 and AOM2). Both AOMs are set to generate strong first-order diffracted beams at $f_1 \approx f_2 = f_0 + 100$ MHz, while the zeroth orders are dumped. Both arms are reflected by mirrors to intersect at angle $2\theta$ on the stage-mounted wafer, generating an interference fringe pattern with period $p = \lambda/(2 \sin \theta)$. Close to the wafer each beam is sampled by a weak pickoff splitter. Each of the two picked-off beams is then combined with one-half of the reference beam ($f_R$). Thus two 20 MHz heterodyne signals are generated, which are then guided through fibers to their corresponding phase meters, PM1 and PM2. The latter consist of photodiodes and high-speed signal processing electronics with a digital phase output resolution of $2\pi/512$ and a frequency range of 27.8 MHz centered around 20 MHz.[10] The phase readings $\phi_1$ and $\phi_2$ from PM1 and PM2, respectively, are compared by a digital signal processor (DSP/comparator),[12] which then calculates the change in the driving frequency of AOM1 that is necessary to keep the phase difference $\Delta\phi = \phi_2 - \phi_1$ constant at some arbitrary preset value. The three digital frequency synthesizers share a common reference clock and are based on the Analog Devices AD9852 chip. We currently use only the highest 32 bits out of the 48-bit frequency words (frequency resolution $\approx 20$ mHz) for $f_1$, $f_2$, and $f_R$, and 12-bit words for the power settings used to run three independent rf amplifiers, each of which drives one AOM. The fused quartz AOMs have a bandwidth of 50 MHz centered around 105 MHz. Since a fringe drift of one period $p$ per second corresponds to a frequency difference of 1 Hz between the two interfering arms, one can in principle control fringe movement up to a rate of more than $2.5 \times 10^7$ periods/s.

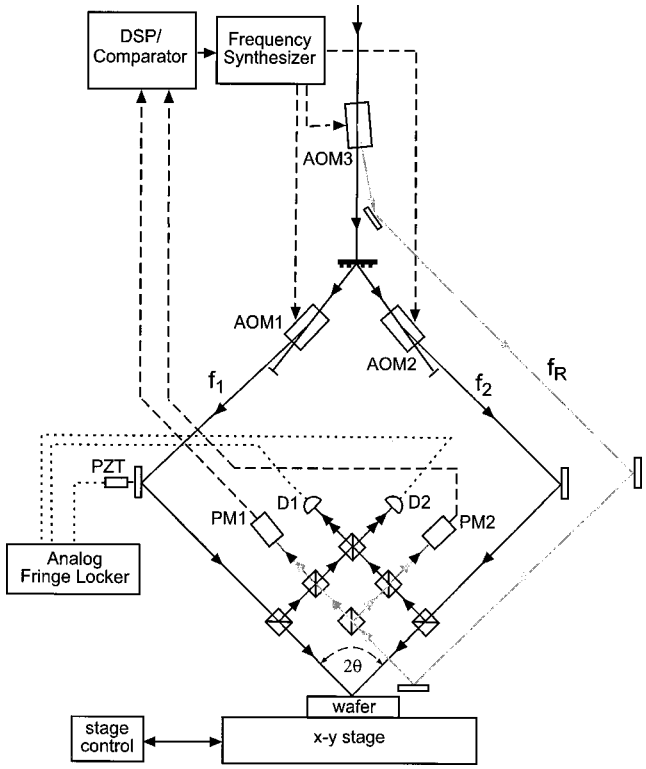


FIG. 2. Schematic of the digital heterodyne fringe locking system. Components not needed for the "reading" of gratings (see Fig. 5) are omitted for clarity.

In order to allow a performance comparison, a commercially available analog fringe-locking system (AFL) is included in the setup.[14] Parts of the two picked-off beams are combined into two overlapping pairs through a dielectric beam splitter. The resulting homodyne signals, which are out of phase by $\pi$ with respect to each other, are detected by photodiodes D1 and D2.[15] The analog feedback electronics actuate the piezo-mounted mirror to equalize the intensities measured at D1 and D2.

The *x*-*y* stage that holds the substrate is also heterodyne interferometer controlled, using the same type of electronics as for the heterodyne phase meters, but with a HeNe laser ($\lambda = 633$ nm) and a nominal position resolution of 0.31 nm.[10]

## III. EXPERIMENTAL RESULTS

Without feedback control the phase difference $\Delta\phi$ typically varies over $\pi$ within 10 s. This corresponds to a fringe drift of $p/2$, which would lead to a complete loss of contrast.

### A. Analog fringe locker

First we evaluate the performance of the analog fringe locker in our system, using the high-resolution digital phase-sensing electronics. It is possible to reduce the intensity of the reference beam to the point where it does not impede the measurement at D1 and D2 and still obtain a sufficiently strong heterodyne signal at PM1 and PM2. In this mode $\Delta\phi$ can be digitally measured while only the analog feedback loop is closed. As can be seen from the gray line in Fig. 3, $\Delta\phi/2\pi$ varies within $\pm p/20$ peak-to-peak in agreement with the specifications for the analog system. This performance is a lower limit, since the AFL locks to the signals detected at D1 and D2, which have traversed slightly different paths than the signals at PM1 and PM2. The intensity fluctuations directly measured on D1 with a 0–45 kHz bandwidth amplifier and oscilloscope actually appear closer to $\pm p/30$ than $\pm p/20$.

### B. Digital heterodyne fringe locker

The feedback loop currently employed in the digital heterodyne system uses simple proportional control. For example, if locking to the condition $\Delta\phi = 0$ is desired, then

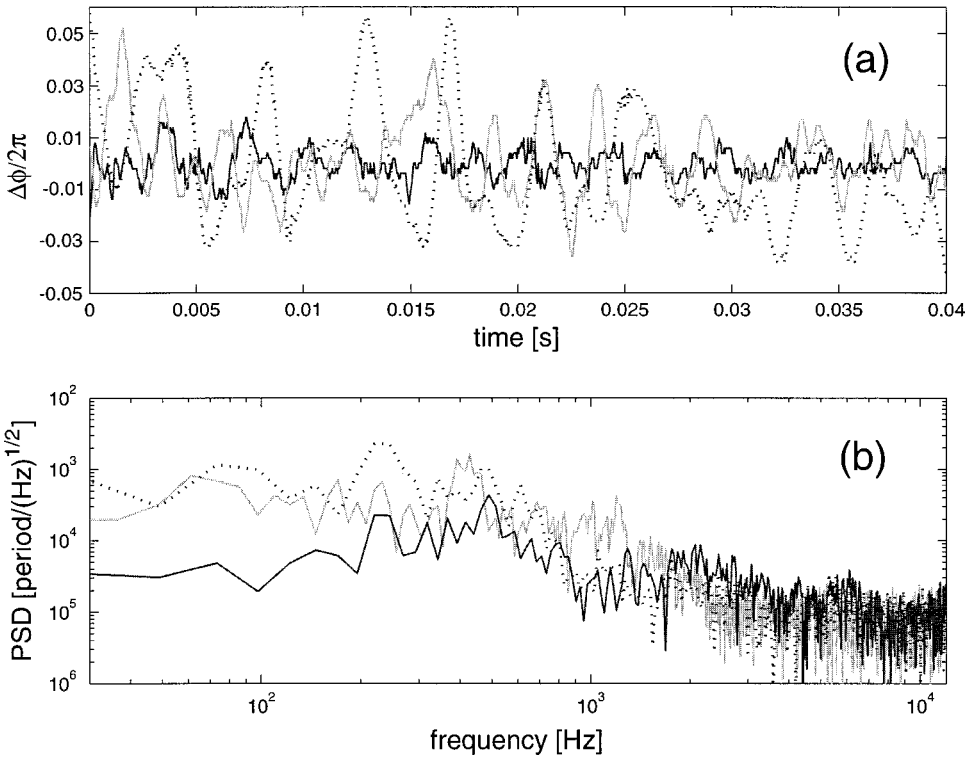


FIG. 3. (a) Comparison of typical fringe drift (in fractions of a fringe period $p=\Delta\phi/2\pi$) without locking (dotted line), with the analog fringe locker (gray line), and with the digital fringe locker (solid black line) over 40 ms. (b) Power spectral density for the data from (a).

$f_2-f_1=0$, and the DSP sets the rf frequency for AOM1 to $F_C+K\Delta\phi$, where $F_C$ is the nominal center frequency for AOM1 and AOM2, and $K$ is experimentally found to be around 1400 Hz/rad for optimum disturbance rejection. The frequency for AOM1 is updated at a 25 kHz rate, while the frequency for AOM2 remains at $F_C$.

With only the digital loop closed a significant improvement in performance is observed (black solid line in Fig. 3). $\Delta\phi/2\pi$ varies peak-to-peak by $\pm p/60\approx\pm 3\sigma$, and the power spectral density is reduced up to a frequency close to the value of $K$. Since the feedback algorithm can be improved and the speed of the electronics has not yet been fully exploited we expect that further significant reductions in phase error are possible.

It should be noted that a change in the AOM rf drive frequency also leads to a change in the angle between the zeroth-order and the first-order diffracted beams, $2\theta_{AO}\approx\lambda F_C/(nv_s)$. Here $F_C=100$ MHz, the index of refraction $n\approx 1.5$ in fused quartz, and the sound velocity is $v_s=5960$ m/s. Any variation in the incident angle at the substrate changes the period of the interference pattern. However, for the data from Fig. 3 the changes in drive frequency for AOM1 are within $\approx\pm 100$ Hz, i.e., the fractional change in the period of the interference pattern is only $\pm\Delta p/p\approx\pm 5\times 10^{-9}$. For periods on the order of a few hundred nanometers this effect is negligible compared to the fringe motion that we can tolerate. However, when scanning at high speed as shown in Fig. 1(b) the interference angle between the two arms will have to be held constant through actuation of additional steering mirrors.

The performance of the heterodyne fringe locking system is currently also limited by environmental factors. The system is situated inside a clean room on a simple breadboard that sits above a vibration isolated granite slab. However, the ceiling air blowers above the breadboard add a significant acoustic load to the noisy laboratory environment. With those blowers turned off the peak-to-peak fluctuations during fringe-locking improved to $\pm 3\sigma=\pm p/100$ (see Fig. 4).

Since phases are not measured directly at the substrate, differential phase changes along the short air paths between substrate and phase meters can compromise locking performance at the substrate. These effects need to be minimized through symmetric design and a well-controlled environment.

## IV. OUTLOOK AND SUMMARY

The digital heterodyne fringe control system described above has further powerful features that might make it attractive for applications outside of SBIL. Instead of only one AOM, both AOMs can be actively controlled. Also the phase difference $\Delta\phi$ can be locked at any value, and the frequency synthesizers can change phase and frequency independently.

For use in SBIL we plan to add information about the stage position, supplied by the stage interferometer electronics, into the feedback loop in order to keep the fringes locked to the moving substrate. This requires accurate knowledge of the fringe period $p$. The necessary metrology for this task is described in a separate article.[12] Also, for a goal of 1 nm phase distortion across a 30 cm grid it is necessary to include corrections due to relativistic effects at stage speeds as low as a few cm/s.[16] Furthermore, digital control of the AOM rf power will enable convenient real-time balancing of light intensity in the two arms for maximum fringe contrast.

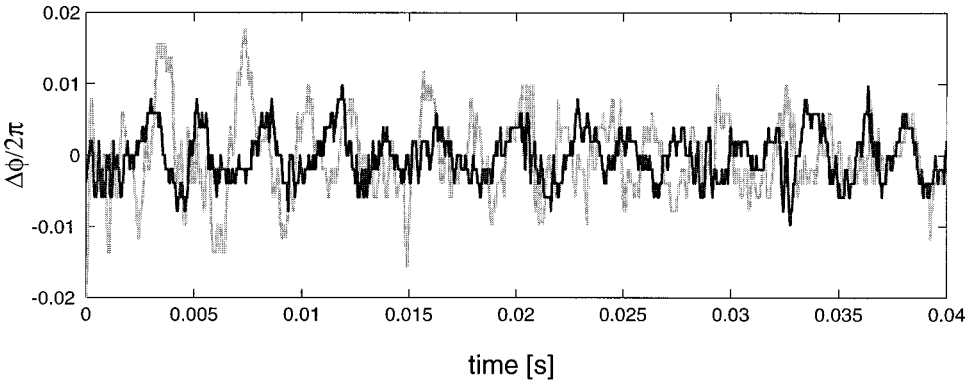


FIG. 4. Typical fringe drift (in fractions of a fringe period $p=\Delta\phi/2\pi$) in the normal clean room environment (gray line) and with reduced acoustic load (solid black line, blowers turned off). On this scale the resolution of the digital electronics ($1/512 \approx 0.002$) is already discernible.

The system shown in Fig. 2 can be extended to enable heterodyne ''reading'' of phase information from an existing grating that is scanned through the interference region (see Fig. 5). For that purpose $p$ should be close to the grating period, and the grating should be closely aligned with the interference fringe pattern. The frequencies $f_1$ and $f_2$ now differ by some fixed amount (e.g., 20 MHz). Again two different phase signals are compared. One signal consists of the superposition of the reflected beam from one arm and the back-diffracted beam from the other arm (PM3), while the other signal is the superposition of beams from each arm, picked off close to the grating (PM4). The difference between these heterodyne signals gives intensity-weighted information, averaged over the beam spot, about the phase of the grating as a function of position, assuming that the stage position can be determined independently. This technique can therefore be used to generate phase distortion maps for any given grating.

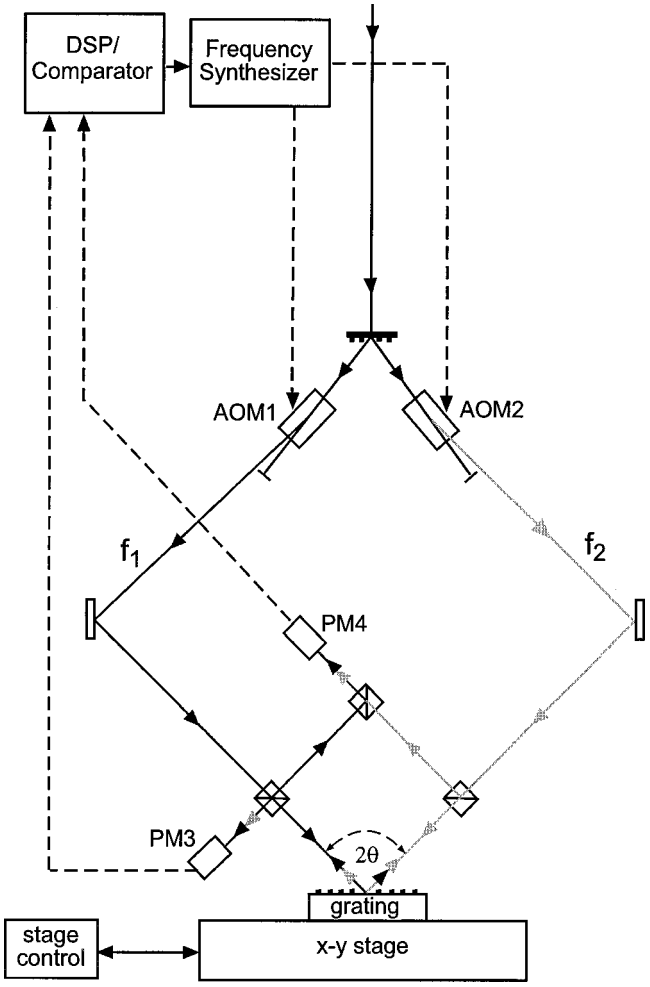


FIG. 5. Schematic of the SBIL reading mode. Components not needed for the SBIL writing mode (see Fig. 2) are omitted for clarity.

In summary we have designed and implemented a digital heterodyne interference fringe control system for use in scanning-beam interference lithography. The initial proof-of-principle system has achieved fringe locking to within $\pm p/100$ peak-to-peak. We expect its performance to be improved in the near future. A soon-to-be-installed environmental enclosure will advance control of environmental variables (temperature, pressure, humidity, etc.) by orders of magnitude and better insulate the SBIL system acoustically. The feedback control algorithm can be improved, and we expect to be able to update the feedback loop at several hundred kHz. These improvements should allow us to keep the phase error very close to the phase resolution of the electronics at $\pm 2\pi/512$. Configurations with higher phase resolution are available if necessary.[17]

## ACKNOWLEDGMENTS

The authors gratefully acknowledge outstanding technical support from E. Murphy and B. Fleming. This work was supported by the Defense Advanced Research Projects Agency (DARPA) under Grant No. DAAG55-98-1-0130 and the National Aeronautics and Space Administration (NASA) under Grant No. NAG5-5271.

[1]D. B. Neumann and H. W. Rose, Appl. Opt. **6**, 1097 (1967).
[2]G. Saxby, *Practical Holography* (Prentice Hall, New York, 1988).
[3]D. R. MacQuigg, Appl. Opt. **16**, 291 (1977).
[4]A. A. Freschi and J. Frejlich, Opt. Lett. **20**, 635 (1995).
[5]M. Sato, K. Seino, K. Onodera, and N. Tanno, Opt. Commun. **184**, 95 (2000).
[6]A. Brozeit, J. Burke, and H. Helmers, Opt. Commun. **173**, 95 (2000).
[7]See, for example, A. Yariv, *Optical Electronics in Modern Communications*, 5th ed. (Oxford University Press, New York, 1997).
[8]K. Oka, M. Tsukada, and Y. Ohtsuka, Meas. Sci. Technol. **2**, 106 (1991).
[9]N. M. Oldham, J. A. Kramar, P. S. Hetrick, and E. C. Teague, Precis. Eng. **15**, 173 (1993).

[10]F. C. Demarest, Meas. Sci. Technol. **9**, 1024 (1998).
[11]M. L. Schattenburg, C. Chen, P. N. Everett, J. Ferrera, P. Konkola, and H. I. Smith, J. Vac. Sci. Technol. B **17**, 2692 (1999).
[12]C. G. Chen, P. T. Konkola, R. K. Heilmann, G. S. Pati, and M. L. Schattenburg, J. Vac. Sci. Technol. B, these proceedings.
[13]P. T. Konkola, C. G. Chen, R. K. Heilmann, and M. L. Schattenburg, J. Vac. Sci. Technol. B **18**, 3282 (2000).
[14]Stabilock II® Active Fringe Stabilizer, Odhner Holographics, Amherst, NH.
[15]E. H. Anderson, H. I. Smith, and M. L. Schattenburg, U.S. Patent No. 5142385 (1992).
[16]R. K. Heilmann, P. T. Konkola, C. G. Chen, and M. L. Schattenburg, J. Vac. Sci. Technol. B **18**, 3277 (2000).
[17]J. Lawall and E. Kessler, Rev. Sci. Instrum. **71**, 2669 (2000).